Simple Figure of Merit for Diodes in Optical Rectennas

Saumil Joshi and Garret Moddel, *Senior Member, IEEE*

***Abstract*—Harvesting infrared and visible light energy using optical rectennas—diode-coupled optical antennas—is strongly dependent on the diode current–voltage characteristics. Predicting the conversion efficiency is an arduous procedure that involves calculating the efficiency by solving the nonlinear diode circuit using the theory of photon-assisted tunneling (PAT). Because of the complexity of the calculations, many rectenna diodes have been reported without indications of how well these diodes will actually function in a rectenna. To provide a quick assessment of the diodes' usefulness in optical rectennas, we provide a figure of merit (*FOM*) that incorporates the diodes' current–voltage and capacitance, the antenna radiation resistance, and the illumination parameters.**

***Index Terms*—Photon-assisted tunneling (PAT), photovoltaics, rectennas, solar cell, tunneling.**

I. Introduction

An optical rectenna consists of an antenna that receives high-frequency electromagnetic radiation, connected to a high-speed diode that rectifies the ac currents to dc. Rectennas have been proposed for energy harvesting in the IR and for optical detection [1]–[4] and use high-speed diodes, such as metal–insulator–metal (MIM) diodes [5]–[11], geometric diodes [12], coupled to metal antennas [13], [14], carbon nanotubes antennas [15], and frequency-selective surfaces [16]. Their analysis is carried out using the quantum theory of photon-assisted tunneling (PAT) applied to the diode [17], [18] and requires solving the currents and voltages in a nonlinear equivalent electrical circuit [19], which is complex and time-consuming. In this paper, we propose a simple figure of merit (*FOM*) to estimate the rectification efficiency of a rectenna under monochromatic illumination based on measured or simulated diode characteristics and the input conditions.

Several parameters determine the performance of the rectenna, including diode parameters, antenna parameters, and the input conditions. We calculate the effect of the different parameters on rectenna efficiency, determined using PAT theory, and the results correspond well with the *FOM* calculations. Then, we demonstrate the calculation of the *FOM* using step metal–insulator–insulator–metal (MIIM) diodes and resonant MIIM diodes [20]–[22]. The *FOM* provides a convenient and qualitative expression to estimate the rectenna's performance.

Manuscript received July 25, 2015; revised December 13, 2015; accepted March 8, 2016. Date of publication April 4, 2016; date of current version April 19, 2016. This work was carried out under a contract from RedWave Energy Inc.

S. Joshi was with the University of Colorado, Boulder, CO 80309 USA. He is now with the Department of Electrical and Computer Engineering, University of Massachusetts, Amherst, MA 01003 USA (e-mail: joshi.saumil@gmail.com).

G. Moddel is with the Department of Electrical, Computer, and Energy Engineering, University of Colorado, Boulder, CO 80309 USA (e-mail: moddel@colorado.edu).

Color versions of one or more of the figures in this paper are available online at http://ieeexplore.ieee.org.

Digital Object Identifier 10.1109/JPHOTOV.2016.2541460

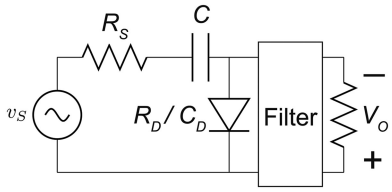

Fig. 1. Schematic of the rectenna circuit. The antenna is represented by the source voltage v_S and radiation resistance R_S. The capacitor *C* provides voltage clamping and models dc current blocking by the antenna. The low-pass filter blocks the ac power from being dissipated in the load, the dc operating voltage across which is V_O. The diode resistance and capacitance are represented by R_D and C_D, respectively.

II. Parameters Determining Rectenna Performance

There are six parameters that determine the performance of a rectenna system and appear in the expression of the *FOM*. They can be divided into three categories.

1) *Input conditions:* power at the antenna terminals ($P_{\rm in}$) and the frequency ($f = \omega/2\pi$) of the incoming electromagnetic wave;
2) *Diode characteristics:* diode area (A_D), capacitance (C_D), forward resistance (R_f), and reverse resistance (R_r) in the form of the current density [*J(V)*] characteristics of the diode, determined by approximating the diode *I(V)* by a piecewise linear characteristic;
3) *Antenna parameters:* radiation resistance (R_S) of the antenna, where we assume that the coupling efficiency between free-space and the antenna is unity, the antenna is in resonance (so that its impedance is purely resistive), and the propagation of the surface plasmons from the antenna to the diode is lossless.

The rectenna schematic is shown in Fig. 1. As will be shown, the rectenna performance depends on the input conditions, which means that the rectenna and the diode have to be designed based on the application. The six parameters determining the *FOM* of the rectenna can be grouped into three recognizable terms.

1) *Diode reverse leakage power:* The reverse leakage power ($P_{\rm leak}$) is the dc power lost due to the flow of finite reverse leakage current ($I_{\rm leak}$) in the diode at the operating voltage (V_O) of the rectenna. Since the rectenna operates in the second quadrant of the diode *I(V)*, the diode reverse leakage current at V_O flows in the opposite direction to the dc illuminated current ($I_{\rm illum}$) and, therefore, degrades rectenna performance [23]. The $P_{\rm leak}$ at the V_O due to the

reverse leakage current is

$$P_{\rm leak} = V_O I_{\rm leak}. \tag{1}$$

A good energy harvesting diode has a leakage current such that $P_{\rm in}/P_{\rm peak} \gg 1$.

2) *Diode responsivity:* For efficient rectification, the diode must be asymmetric around the rectenna V_O and have a large responsivity [24]. The diode current responsivity, which is the dc current out per unit ac power in, can be written as

$$\beta_\Delta = \frac{1}{\Delta}\left(\frac{I(V_O+\Delta) - 2I(V_O) + I(V_O-\Delta)}{I(V_O+\Delta) - I(V_O-\Delta)}\right). \tag{2}$$

Here, the Δ is a step voltage that depends on the operating regime of the rectenna. Although the diode voltage amplitude (V_D) is the relevant parameter, due to its dynamic nature and dependence on V_O, we use V_S as an approximation for V_D to determine the operating regime. We approximate Δ by the source voltage (V_S) if the rectenna operates in the classical regime ($V_S \gg \hbar\omega/q$) and is equal to $\hbar\omega/q$ if the rectenna is in the quantum regime ($V_S < \hbar\omega/q$) [19]. A formula for determining V_S is given as [25]

$$V_S = \sqrt{8 R_S P_{\rm in}^{\rm AC}}. \tag{3}$$

At optical frequencies, the antenna parameters (resonance frequency, radiation resistance, etc.) do not follow classical antenna theory and might need some modifications [26], but (3) would still apply in estimating the *FOM*.

3) *Coupling efficiency between the antenna and the diode:* The input conditions and the diode *I*(*V*) characteristics determine the diode ac resistance (R_D). For quantum operation, R_D is the secant resistance of the diode because in quantum operation, the oscillating current samples the diode at only two points in its *I(V)* curve [17]. Since calculating the R_D in the classical case is not straightforward, we approximate it using the same expression as the quantum R_D but with a Δ ($= V_S$) suitable for classical operation

$$R_D = \frac{2\Delta}{(V_O+\Delta)/R_f - (V_O-\Delta)/R_r}. \tag{4}$$

The R_D in parallel with R_S determine the effective ac resistance of the system, which along with the C_D gives the *RC* time constant and the cutoff frequency (f_c) of the rectenna

$$f_c = \frac{1}{2\pi \dfrac{R_S R_D}{R_S + R_D} C_D}. \tag{5}$$

The coupling efficiency is written as [27],

$$\eta_C = \frac{\dfrac{4R_S R_D}{(R_S+R_D)^2}}{1 + \left(2\pi f \dfrac{R_S R_D}{R_S + R_D} C_D\right)^2}. \tag{6}$$

The η_C is 100% when $R_S = R_D$ and $f \ll f_c$.

III. Steps to Determine the Figure of Merit

We calculate the *FOM* using the following sequence of six steps.

1) Calculate the input power at the antenna

$$P_{\rm in}^{\rm AC} = \eta_{\rm ant} A_{\rm ant} I_{\rm in}. \tag{7}$$

The $\eta_{\rm ant}$ is the antenna efficiency, $A_{\rm ant}$ is the antenna effective area, and $I_{\rm in}$ is the input intensity. In the absence of information about the antenna, we make the approximation that $\eta_{\rm ant} = 1$.

2) Calculate the voltage across the antenna using (3).
3) Determine if the rectenna operates in the classical regime ($V_S > \hbar\omega/q$) or the quantum regime ($V_S < \hbar\omega/q$).
4) Using the appropriate Δ ($= \hbar\omega/q$ in the quantum regime, and $V_{\rm S}$ in the classical regime) and V_O, estimate the β_Δ using (2) and R_D using (4) assuming, in the classical case, that the diode is piecewise linear. The R_D in the classical regime is an approximation to the diode ac resistance. We recommend a $V_O = -\Delta/2$ as a starting value to approximate the R_D and β_Δ, as we do in the next section. This is not the V_O giving the maximum efficiency of the rectenna but is convenient for comparing the rectenna *FOM* under different conditions. To determine the $V_{\rm O}$ at which the η is maximum, the V_O can be varied to maximize the *FOM,* as we show later when we calculate the *FOM* of MIIM diodes.
5) Calculate the η_C at the V_O using (6).
6) The rectenna *FOM* is now expressed as the combination of the β_Δ, η_C, and $P_{\rm leak}$ as follows:

$$FOM = 100\left(|V_O|\,\beta_\Delta - \frac{|V_O I_{\rm leak}|}{P_{\rm in}^{\rm AC}}\right) \times \eta_C. \tag{8}$$

The expression is such that the *FOM* corresponds approximately to the power conversion efficiency of the rectenna. If the *FOM* < 1, the rectenna design is poor and the efficiency is poor, whereas for *FOM* > 10, the rectenna can be expected to perform well, and the efficiency is >10%. This is shown in the next section where we compare the *FOM* with the efficiency calculated for a rectenna having a piecewise linear diode, under different conditions using PAT theory presented in [19]. In those referenced papers, C_D was assumed to be negligible and had no effect on the rectenna efficiency. Here, we introduce the effect of C_D using an *RC* coupling efficiency term

$$\eta_C^{\rm RC} = \frac{1}{1 + \left(2\pi f \dfrac{R_D R_S}{R_D + R_S} C_D\right)^2}. \tag{9}$$

The overall efficiency, approximated by the *FOM*, is the product of $\eta_C^{\rm RC}$ and the efficiency calculated using PAT theory.

IV. Calculation of the Figure of Merit

To show the correspondence of the *FOM* with the efficiency calculated from PAT, we calculate the rectenna *FOM* versus R_r for different input conditions ($P_{\rm in}$, f) and diode characteristics (C_D, R_f). In each calculation, we change one parameter while

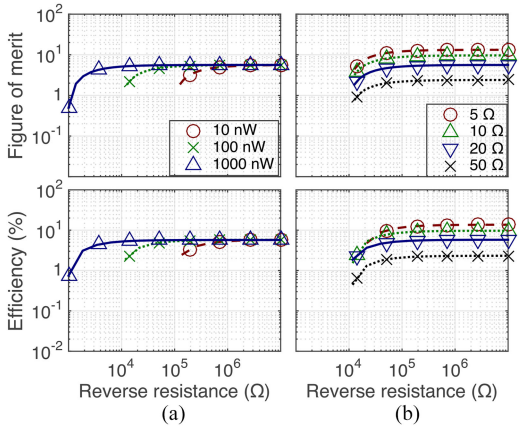

Fig. 2. Plots showing close agreement between the *FOM* and the rectenna energy conversion efficiency (η) versus the diode reverse resistance (R_r), calculated using PAT theory for different input powers ($P_{\rm in}$) and diode forward resistances (R_f). The diode has piecewise linear *I(V)* characteristics. (a) Effect of varying $P_{\rm in}$ (10 nW to 1000 nW) on the *FOM* (with $R_f = 20\ \Omega$, $f = 10$ THz, $C_D = 1$ fF). The *FOM* decreases with decrease in the R_r due to the increase in leakage current. (b) Effect of varying R_f (5–50 Ω) on the *FOM* (with $P_{\rm in} = 100$ nW, $f = 10$ THz, $C_D = 1$ fF). As R_f increases, the impedance matching with the antenna at the operating voltage (V_O) gets poorer and the *FOM* decreases. Also plotted below the *FOM* plots is the efficiency calculated using PAT under the same conditions, showing that the efficiency follows the same trend as the *FOM*.

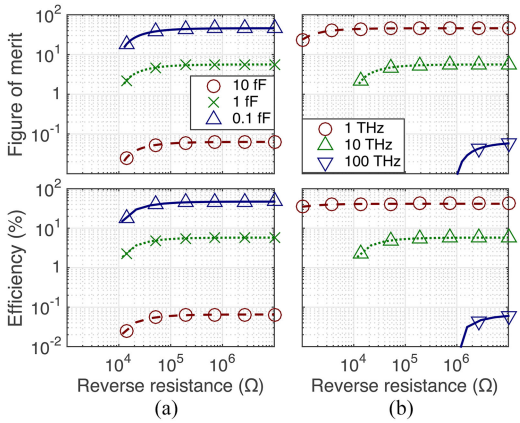

Fig. 3. Plots of the *FOM* versus R_r and the corresponding rectenna efficiency calculated using PAT, showing a correlation between the two, for varying C_D and *f*. (a) Effect of C_D (10 to 0.1 fF) on the *FOM* (with $R_S = 100\ \Omega$, $R_f = 20\ \Omega$, $f = 10$ THz, $P_{\rm in} = 100$ nW). Decreasing C_D increases the *FOM* due to a decrease in the rectenna *RC* time constant. (b) Effect of *f* (1–100 THz) on the *FOM* (for $P_{\rm in} = 100$ nW, $R_S = 100\ \Omega$, $R_f = 20\ \Omega$, $C_D = 1$ fF). Increasing *f* decreases the *FOM* because the V_O becomes more negative, and therefore, the curves shift to the right due to increase in the leakage current relative to the rectified current.

keeping the other parameters the same. The plots of *FOM* versus R_r with changing *f*, C_D, $P_{\rm in}$, and R_f are shown in Figs. 2 and 3. The R_S is assumed to be 100 Ω, required for impedance matching with free space, and as suggested in the previous section, the $V_{\rm O}$ is fixed at half $-\hbar\omega/q$ in the quantum regime and half $-V_S$ in classical regime.

We make the following observations based on the *FOM* calculations.

TABLE I
IMPROVING DIODE PERFORMANCE BASED ON *FOM* PARAMETERS

Term	To increase the *FOM*
β_Δ	Increase *J*(*V*) asymmetry at voltages $V_O \pm \hbar\omega/q$
$I_{\rm leak}$	Decrease leakage current density at V_O, decrease A_D
η_C	Adjust *J*(*V*) and A_D to match R_D with R_S, decrease C_D and increase *J*(*V*) to reduce $1/R_D C_D$ with respect to ω

Parameters that are used in (8) to calculate the *FOM* and their dependence on the diode and input conditions.

1) With decreasing $P_{\rm in}$, the *FOM* degrades at low values of R_r [see Fig. 2(a)] due to the excess leakage current. The $P_{\rm in}$ is varied from 10 to 1000 nW, which is in the range of spatially coherent power available from blackbody sources such as the sun [28].
2) The *FOM* decreases on increasing the R_f [see Fig. 2(b)] due to an increase in the *RC* time constant of the rectenna and an increase in R_D at the V_O, resulting in a poor impedance matching condition.
3) An increase in C_D [see Fig. 3(a)] and an increase in *f* [see Fig. 3(b)] leads to a decrease in the *FOM*, by increasing the effect of the *RC*-limited cutoff frequency of the rectenna.

We also calculate the rectenna efficiency using PAT theory under the same conditions as above. The efficiency results are shown in Figs. 2 and 3 below the *FOM* plots and follow the same trend as the *FOM* with the change in diode and input parameters, showing a very strong correlation between the *FOM* and PAT theory results.

These results show that the *FOM* is a good indicator of the performance of the rectenna, and elaborate calculations are not required to get an approximate idea of its energy harvesting efficiency. In Table I, we summarize the steps that can be taken to increase the *FOM* by adjusting the parameters that directly affect the terms on which the *FOM* depends.

V. FIGURE OF MERIT OF METAL–INSULATOR–INSULATOR–METAL DIODES

We demonstrate the calculation of the *FOM* using a resonant MIIM diode and a step MIIM diode [21]. We use MIIM diodes because they can achieve greater asymmetry, a smaller turn-on voltage and give higher rectification efficiencies compared to single insulator MIM diodes. The diode structure is shown in Fig. 4(a) and (c), and their current density versus voltage [*J*(*V*)] characteristics, determined using the transfer-matrix method presented in [21], are plotted in Fig. 4(b) and (d), respectively.

To see the effect of the reverse leakage current on diode performance in these double-insulator diodes, we first calculate the *FOM* versus V_O characteristics for the resonant MIIM diode with changing diode edge length (for a square-shaped diode)

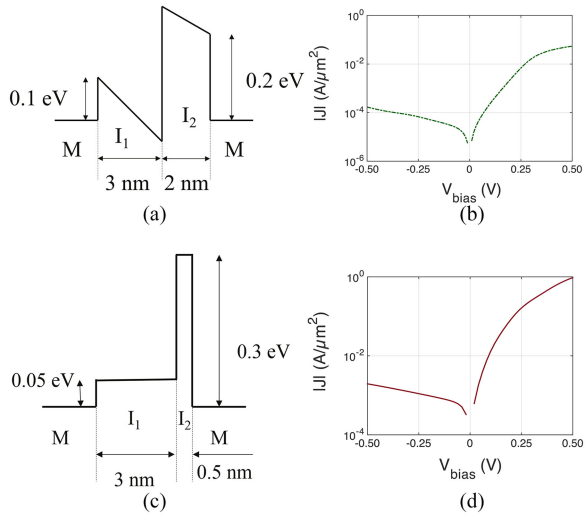

Fig. 4. Energy-band diagram and the calculated current density versus voltage [*J(V)*] characteristics of resonant and step MIIM diodes. (a) Energy-band diagram of the resonant diode for the indicated barrier heights and insulator thicknesses, and a work function difference ($\Delta\varphi$) of 0.2 eV between the two metal layers. The relative permittivity of the two insulators (I_1 and I_2) are 1 and 2, respectively. (b) *J(V)* characteristics of the resonant MIIM diode for the parameters in (a), calculated using the method presented in [21] that uses the transfer matrix method to solve for the Schrodinger equation. (c) Energy-band diagram of the step diode for the barrier heights and insulator thicknesses indicated in the figure. $\Delta\varphi = 0$ eV, and the relative permittivities of I_1 and I_2 are 100 and 1, respectively. (d) *J(V)* characteristics of the step MIIM diode for the conditions given in (c). The effective mass of the electron in the insulators is assumed to be its rest mass.

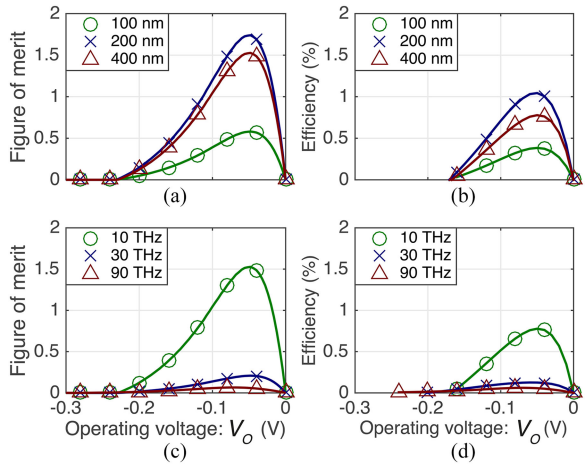

Fig. 5. *FOM* and efficiency (η) characteristics of the resonant MIIM diode in Fig. 4(b), showing the effect of the increase in reverse leakage current with size and operating frequency. The C_D is ~ 2.2 fF/μm^2. (a) *FOM* versus V_O characteristics of the rectenna for increasing diode edge length from 100 to 400 nm keeping $f = 10$ THz, and $P_{\rm in} = 100$ μW. (b) η versus V_O characteristics of the rectenna calculated using PAT theory, and the same conditions as in (a). Both (a) and (b) show that with the increase in diode size, the peak *FOM* and efficiency ($\eta_{\rm peak}$) first increase due to improvement in the η_C but later decrease due to increase in the reverse leakage current. (c) *FOM* versus V_O characteristics for increasing f from 10 to 90 THz keeping an edge length of 400 nm and $P_{\rm in} = 100$ μW. (d) η versus V_O characteristics calculated using PAT theory, under the same conditions as in (c), showing that an increase in the f decreases the coupling efficiency due to the limited *RC* time constant of the diode.

and changing incident frequency. The peak *FOM* increases as the size increases (from 100 to 200 nm) due to increase in coupling efficiency but decreases as the size is increased further (to 400 nm) due to increased reverse leakage current. The results are shown in Fig. 5(a). The η characteristics, in Fig. 5(b), follow the same trend as the *FOM* showing that there is a good correlation between the two. Similar results are seen in Fig. 6(a) and (b), where we plot the *FOM* and η versus V_O characteristics for a step MIIM diode, for increasing diode edge length (50–200 nm).

The effect of increasing frequency is a decrease in the *FOM* and the η due to poor *RC* coupling, following (6). This is shown in Fig. 5(c) and (d) for the resonant MIIM diode and for the step MIIM diode in Fig. 6(c) and (d), where we plot the *FOM* and η versus V_O with increasing f (10–90 THz). Novel antenna designs and architectures such as that proposed recently using carbon nanotube forests in [15] could circumvent these coupling efficiency constraints (η_C approaching 100%). This way, the rectenna efficiency would be limited only by the diode asymmetry and leakage current requirements, giving significantly higher power conversion efficiencies.

Although the *FOM* corresponds only approximately to the PAT efficiency of the rectenna (because the R_D, β_Δ, and $I_{\rm leak}$ are approximated assuming that the diode is piecewise linear), it is a good indicator of the monochromatic efficiency of the rectenna.

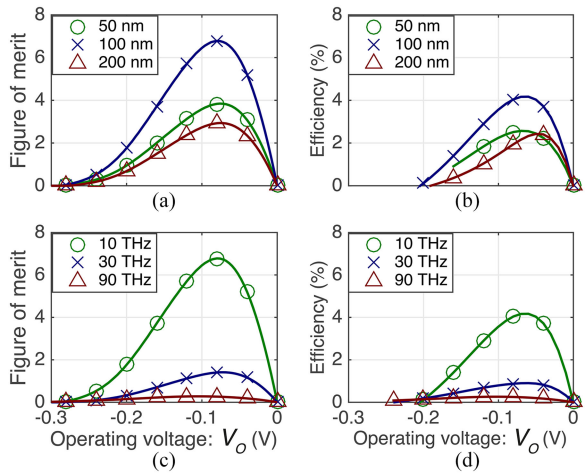

Fig. 6. *FOM* and efficiency (η) versus V_O characteristics for the step MIIM diode shown in Fig. 4 (d), with $C_D \sim 17$ fF/μm^2. The results follow the same trend as the resonant MIIM diode results shown in Fig. 5. (a) *FOM* versus V_O characteristics of the rectenna for increasing diode edge length from 50 to 200 nm, keeping $f = 10$ THz, and $P_{\rm in} = 100$ μW. (b) Efficiency versus V_O characteristics of the rectenna calculated using PAT theory for the same conditions as in (a). (c) *FOM* versus V_O characteristics for increasing f from 10 to 90 THz and keeping an edge length of 100 nm and $P_{\rm in} = 100$ μW. (d) η characteristics calculated using PAT theory under the same conditions as in (c).

VI. Conclusion

In this paper, we have developed a method to calculate the *FOM* of a rectenna. The simple expression for the *FOM* is a combination of the three mechanisms that determine rectenna

performance: the diode reverse leakage power relative to the input power, diode responsivity, and the coupling efficiency between the antenna and the diode. We calculated the *FOM* using different rectenna parameters and input conditions and compared the results with efficiency calculated using PAT theory showing a strong correlation between the two. We demonstrated the application of the *FOM* to double-insulator MIM (MIIM) diodes and showed that the simple expression can be used to provide a good estimate of the rectenna performance under monochromatic illumination.

ACKNOWLEDGMENT

The authors would like to thank Amina Belkadi, Bradley Pelz, and Shuai Yuan for helpful suggestions to improve the manuscript. G. Moddel holds stock in RedWave Energy, Inc.

REFERENCES

[1] A. B. Hoofring, V. J. Kapoor, and W. Krawczonek, "Submicron nickel-oxide-gold tunnel diode detectors for rectennas," *J. Appl. Phys.*, vol. 66, no. 1, pp. 430–437, Jul. 1989.
[2] M. Sarehraz *et al.*, "Rectenna developments for solar energy collection," in *Proc. Conf. Rec. 31st IEEE Photovoltaic Spec. Conf.*, 2005, pp. 78–81.
[3] R. Corkish, M. A. Green, and T. Puzzer, "Solar energy collection by antennas," *Sol. Energy*, vol. 73, no. 6, pp. 395–401, Dec. 2002.
[4] F. Yu, G. Moddel, and R. Corkish, "Quantum rectennas for photovoltaics," in *Advanced Concepts Photovoltaics*, 1st ed., A. J. Nozik, G. Conibeer, and M. C. Beard, Eds. London, U.K.: Royal Soc. Chem., 2014, pp. 506–546.
[5] C. A. Mead, "Operation of tunnel-emission devices," *J. Appl. Phys.*, vol. 32, no. 4, pp. 646–652, Apr. 1961.
[6] C. B. Duke, *Tunneling in Solids*, vol. 10. New York, NY, USA: Academic, 1969.
[7] M. Heiblum, S. Wang, J. Whinnery, and T. Gustafson, "Characteristics of integrated MOM junctions at DC and at optical frequencies," *IEEE J. Quantum Electron.*, vol. QE-14, no. 3, pp. 159–169, Mar. 1978.
[8] B. J. Eliasson, *Metal-Insulator-Metal Diodes for Solar Energy Conversion*. Boulder, CO, USA: Univ. Colorado, 2001.
[9] P. Periasamy *et al.*, "Fabrication and Characterization of MIM diodes based on Nb/Nb2O5 Via a rapid screening technique," *Adv. Mater.*, vol. 23, no. 27, pp. 3080–3085, Jul. 2011.
[10] K. Choi *et al.*, "A focused asymmetric metal-insulator-metal tunneling diode: Fabrication, DC characteristics and RF rectification analysis," *IEEE Trans. Electron Devices*, vol. 58, no. 10, pp. 3519–3528, Oct. 2011.
[11] N. M. Miskovsky *et al.*, "Nanoscale devices for rectification of high frequency radiation from the infrared through the visible: A new approach," *J. Nanotechnol.*, vol. 2012, pp. 1–19, 2012.
[12] Z. Zhu, S. Joshi, S. Grover, and G. Moddel, "Graphene geometric diodes for terahertz rectennas," *J. Phys. Appl. Phys.*, vol. 46, no. 18, May 2013, Art. no. 185101.
[13] J. A. Bean, A. Weeks, and G. D. Boreman, "Performance optimization of antenna-coupled tunnel diode infrared detectors," *IEEE J. Quantum Electron.*, vol. 47, no. 1, pp. 126–135, Jan. 2011.
[14] Z. Ma and G. A. E. Vandenbosch, "Optimal solar energy harvesting efficiency of nano-rectenna systems," *Sol. Energy*, vol. 88, pp. 163–174, Feb. 2013.
[15] A. Sharma, V. Singh, T. L. Bougher, and B. A. Cola, "A carbon nanotube optical rectenna," *Nat. Nanotechnol.*, vol. 10, no. 12, pp. 1027–1032, Dec. 2015.
[16] E. C. Kinzel *et al.*, "Design of an MOM diode-coupled frequency-selective surface," *Microw. Opt. Technol. Lett.*, vol. 55, no. 3, pp. 489–493, Mar. 2013.
[17] S. Grover, S. Joshi, and G. Moddel, "Quantum theory of operation for rectenna solar cells," *J. Phys. Appl. Phys.*, vol. 46, no. 13, Apr. 2013, Art. no. 135106.
[18] J. W. Haus, D. de Ceglia, M. A. Vincenti, and M. Scalora, "Quantum conductivity for metal–insulator–metal nanostructures," *J. Opt. Soc. Amer. B*, vol. 31, no. 2, p. 259, Feb. 2014.
[19] S. Joshi and G. Moddel, "Rectennas at optical frequencies: How to analyze the response," *J. Appl. Phys.*, vol. 118, no. 8, Aug. 2015, Art. no. 084503.
[20] P. Maraghechi, A. Foroughi-Abari, K. Cadien, and A. Y. Elezzabi, "Enhanced rectifying response from metal-insulator-insulator-metal junctions," *Appl. Phys. Lett.*, vol. 99, no. 25, Dec. 2011, Art. no. 253503.
[21] S. Grover and G. Moddel, "Engineering the current–voltage characteristics of metal–insulator–metal diodes using double-insulator tunnel barriers," *Solid-State Electron.*, vol. 67, no. 1, pp. 94–99, Jan. 2012.
[22] N. Alimardani and J. F. Conley, Jr., "Step tunneling enhanced asymmetry in asymmetric electrode metal-insulator-insulator-metal tunnel diodes," *Appl. Phys. Lett.*, vol. 102, no. 14, Apr. 2013, Art. no. 143501.
[23] G. Moddel, "Will rectenna solar cells be practical?" in *Rectenna Solar Cells*, G. Moddel and S. Grover, Eds. New York, NY, USA: Springer, 2013, pp. 3–24.
[24] J. R. Tucker and M. J. Feldman, "Quantum detection at millimeter wavelengths," *Rev. Mod. Phys.*, vol. 57, no. 4, pp. 1055–1113, Oct. 1985.
[25] S. J. Orfanidis, *Electromagnetic Waves and Antennas*. New Brunswick, NJ, USA: Rutgers Univ., 2002.
[26] R. L. Olmon and M. B. Raschke, "Antenna–load interactions at optical frequencies: impedance matching to quantum systems," *Nanotechnol.*, vol. 23, no. 44, p. 444001, 2012.
[27] A. Sanchez, C. F. Davis, K. C. Liu, and A. Javan, "The MOM tunneling diode: Theoretical estimate of its performance at microwave and infrared frequencies," *J. Appl. Phys.*, vol. 49, no. 10, pp. 5270–5277, Oct. 1978.
[28] H. Mashaal and J. M. Gordon, "Fundamental bounds for antenna harvesting of sunlight," *Opt. Lett.*, vol. 36, no. 6, pp. 900–902, Mar. 2011.

Saumil Joshi (S'09) received the B.E. degree in electrical engineering from the University of Delhi, New Delhi, India, in 2009 and the M.S. and Ph.D. degrees in electrical engineering from the University of Colorado, Boulder, CO, USA, in 2011 and 2015, respectively.

Since 2015, he has been a Postdoctoral Researcher with the Department of Electrical and Computer Engineering, University of Massachusetts, Amherst, MA, USA. His research interests include electron transport at the nanoscale, electron tunneling devices for high-speed electronics and memory applications, ionic-electronic devices for neuromorphic computing, and rectennas for energy harvesting and optical detection.

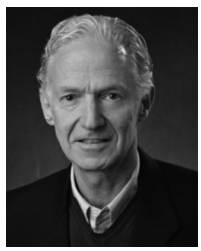

Garret Moddel (SM'93) was born in Dublin, Ireland. He received the B.S.E.E. degree from Stanford University, Stanford, CA, USA, in 1976 and the M.S. and Ph.D. degrees in applied physics from Harvard University, Cambridge, MA, USA, in 1978 and 1981, respectively.

After graduation, he became a founding employee with SERA Solar Corp: a Silicon Valley photovoltaics start-up company. He joined the University of Colorado, Boulder, CO, USA, in 1985, where he is currently a Professor of electrical, computer, and energy engineering. At the University of Colorado, he has developed new thin-film optoelectronic materials and devices. Currently, his research group is involved with quantum engineering of new thin-film metal devices for energy conversion and detection. He was the founding President and CEO of Phiar Corporation: a venture-capital-backed high-tech start-up developing ultrahigh-speed metal–insulator electronics.

Prof. Moddel was named the first CU Inventor of the Year in the Physical Sciences in 2002. He is a Fellow of the Optical Society of America.